Cancer Cell
Article

The Histone Demethylase KDM1A Sustains the Oncogenic Potential of MLL-AF9 Leukemia Stem Cells

William J. Harris,[1] Xu Huang,[1] James T. Lynch,[1] Gary J. Spencer,[1] James R. Hitchin,[2] Yaoyong Li,[3] Filippo Ciceri,[1] Julian G. Blaser,[1] Brigit F. Greystoke,[1] Allan M. Jordan,[2] Crispin J. Miller,[3] Donald J. Ogilvie,[2] and Tim C.P. Somervaille[1,*]
[1]Cancer Research UK Leukaemia Biology Laboratory
[2]Cancer Research UK Drug Discovery Unit
[3]Cancer Research UK Applied Computational Biology and Bioinformatics Group
Paterson Institute for Cancer Research, University of Manchester, Manchester, M20 4BX, United Kingdom
*Correspondence: tsomervaille@picr.man.ac.uk
DOI 10.1016/j.ccr.2012.03.014

SUMMARY

Using a mouse model of human MLL-AF9 leukemia, we identified the lysine-specific demethylase KDM1A (LSD1 or AOF2) as an essential regulator of leukemia stem cell (LSC) potential. KDM1A acts at genomic loci bound by MLL-AF9 to sustain expression of the associated oncogenic program, thus preventing differentiation and apoptosis. In vitro and in vivo pharmacologic targeting of KDM1A using tranylcypromine analogs active in the nanomolar range phenocopied *Kdm1a* knockdown in both murine and primary human AML cells exhibiting *MLL* translocations. By contrast, the clonogenic and repopulating potential of normal hematopoietic stem and progenitor cells was spared. Our data establish KDM1A as a key effector of the differentiation block in MLL leukemia, which may be selectively targeted to therapeutic effect.

INTRODUCTION

Epigenetic dysfunction has a central role in the pathology of myeloid malignancy. This is illustrated by the discovery of recurrently occurring mutations targeting genes that code for epigenetic regulators, such as the methylcytosine hydroxylase TET2, DNA methyltransferase DNMT3A, histone H3K27 methyltransferase EZH2, and Polycomb-related protein ASXL1. Mutations in IDH1 and IDH2 likely also affect the epigenome through neomorphic generation of 2-hydroxyglutarate, which inhibits TET2 and Jumonji-domain histone demethylases. Further, subtypes of acute myeloid leukemia (AML) exhibit distinct and abnormal patterns of DNA methylation (reviewed in Fathi and Abdel-Wahab, 2012).

Novel oncoproteins generated by recurrently occurring chromosomal translocations in myeloid leukemia also induce epigenetic dysfunction. For example, the gene coding for the H3K4 methyltransferase MLL, itself a key epigenetic regulator, is mutated by translocation in about 4% of human AML. This results in constitutive transcription at MLL target genes through aberrant recruitment by MLL fusion partners of proteins and complexes associated with transcription elongation, including pTEFb, PAFc, and DOT1L, an H3K79 methyltransferase (Yokoyama et al., 2010; Lin et al., 2010; Muntean et al., 2010).

These and other observations have led to speculation that regulators of the structure and function of chromatin, such as enzymes that regulate turnover of DNA methylation, histone methylation, or histone acetylation, might be attractive therapeutic targets in myeloid malignancy. To date, only the DNA demethylating agent azacitidine has provided a survival benefit in phase III trials in patients with high-risk myelodysplasia (Fenaux et al., 2009). Although this emphasizes that epigenetic therapies hold significant potential, it also highlights the necessity for identification and evaluation of other therapeutic targets.

Significance

Epigenetic therapies hold promise in the treatment of myeloid malignancy but few targets have been identified and evaluated. Our observations delineate the histone demethylase KDM1A as an enzymatic target to effect downregulation of the MLL-associated oncogenic program and cellular oncogenic potential. The finding that potent pharmacologic inhibitors of KDM1A abrogate clonogenic potential and induce differentiation of both murine and primary human MLL leukemia cells, both in vitro and in vivo, while sparing normal repopulating cells, provides strong evidence for a possible therapeutic window. Our data suggest that KDM1A is a candidate target for differentiation therapy in the MLL molecular subtype of human myeloid leukemia and mandate evaluation of KDM1A inhibition as a therapeutic strategy more generally in myeloid malignancy.

One such candidate is KDM1A (also known as AOF2, LSD1, KIAA0601, or BHC110), a flavin adenine dinucleotide (FAD)-dependent lysine-specific demethylase with monomethyl- and dimethyl-histone H3 lysine-4 (H3K4) and lysine-9 (H3K9) substrate specificity (Shi et al., 2004; Metzger et al., 2005). It is a component of both an MLL supercomplex (Nakamura et al., 2002), which is associated with sites of active transcription, and an ELL (elongation factor RNA polymerase II) complex, which contains pTEFb components that interact with AF9 and AF4, two common oncogenic fusion partners for MLL (Biswas et al., 2011). It is also a component of complexes associated with transcription repression, such as CoREST-HDAC, CtBP, and NuRD (reviewed in Hou and Yu, 2010). Although KDM1A expression has been correlated with poor prognosis in high-risk prostate and breast cancer and poor differentiation in neuroblastoma (Kahl et al., 2006; Schulte et al., 2009; Lim et al., 2010), there is little information to date as to its functional role in myeloid leukemia nor whether it represents a viable therapeutic target.

RESULTS

Kdm1a Is Required for the Clonogenic and LSC Potential of MLL-AF9 AML Cells

To determine whether the expression of known or candidate histone demethylases correlates with AML LSC potential, we analyzed microarray data sets from 23 murine MLL leukemias with known AML colony-forming cell (AML-CFC) frequencies, including those with high (MLL-AF9 and MLL-ENL) or low (MLL-AF10, MLL-AF1p and MLL-GAS7) frequencies (Somervaille et al., 2009). The formation of blast-like (type 1) colonies in semi-solid culture by murine MLL-AF9 AML-CFCs directly correlates with LSC potential (Somervaille and Cleary, 2006). The strongest correlation of array expression values with AML-CFC frequency was observed for *Kdm1a* (Figure S1A and Table S1 available online), and this was confirmed by quantitative PCR (Figure S1B). With the exception of MLL-AF1p AMLs, which exhibit a more myeloproliferative morphologic phenotype than do the other MLL subtypes (Somervaille et al., 2009), FACS-purified KIT^+ cell populations, which are enriched for LSCs (Somervaille and Cleary, 2006; Krivtsov et al., 2006), expressed higher levels of *Kdm1a* than did their downstream KIT^{neg} progeny (Figure S1C), suggesting downregulation of expression upon LSC differentiation. We therefore hypothesized that *Kdm1a* is a key regulator of MLL LSCs.

To address this hypothesis, we generated a cohort of mice with MLL-AF9 AML using a retroviral transduction and transplantation approach (Somervaille et al., 2009) and targeted *Kdm1a* for knockdown (KD) in AML cells from sick mice. *Kdm1a* KD AML cells formed significantly fewer colonies in semi-solid culture compared with cells infected with a nontargeting control (NTC) vector (Figure 1A). The small number of *Kdm1a* KD colonies that did form exhibited altered morphology. Compared with controls, there was a significantly higher frequency of type 3 colonies, which contain terminally differentiated macrophages, and a significantly lower frequency of type 1 colonies, which contain poorly differentiated myeloblasts (Figures 1A and 1B). Cytospin preparations of cells recovered at the end of culture confirmed these observations (Figure S1D). The extent of *Kdm1a* KD correlated significantly with loss of AML-CFC potential, both when separate targeting constructs were compared one with another (Figure 1C) and when a single targeting construct was used with GFP as a selectable marker and transduced cell populations were sorted according to GFP expression (Figures S1E–S1G). Consistent with loss of AML-CFC potential, *Kdm1a* KD cells expressed lower levels of genes associated with MLL LSC potential (Figure 1D). Annexin V binding assays also demonstrated that some *Kdm1a* KD cells underwent apoptosis, beginning at 72–96 hr (Figures S1H and S1I). Loss of AML-CFC potential was also observed with *Kdm1a* KD in murine MLL-ENL, MLL-AF10, MLL-LAF4, and MLL-AF1p leukemia cells (Figure S1J). Forced expression of human *KDM1*A, which differs by three bases to murine *Kdm1a* at the locus targeted by shRNA #4, in significant part rescued CFC potential and blocked differentiation (Figures 1E–1G). Forced expression of h*KDM1A* in leukemias with lower frequencies of LSC, such as those initiated by MLL-AF10 and MLL-AF1p, did not increase AML-CFC frequency (data not shown).

To confirm *Kdm1a* KD AML cells were unable to function as LSCs, we performed secondary transplantation of *Kdm1a* KD or control MLL-AF9 AML cells. All mice (n = 5) receiving 2,000 control AML cells died of short latency AML, as did two of five mice transplanted with 500 cells (Figure 1H). AML cells recovered from sick mice were $Mac1^+Gr1^+GFP^+$, consistent with expression of the NTC lentiviral vector (Figure S1K). By contrast, all mice receiving 500 *Kdm1a* KD AML cells survived to the termination of the experiment, as did three of five mice receiving 2,000 *Kdm1a* KD cells. Of the two mice that received *Kdm1a* KD cells that died, cells from one could not be analyzed due to putrefaction; the other died of a GFP^- leukemia, which expressed normal levels of KDM1A (Figure S1K). Two further cohorts of mice were analyzed for engraftment of GFP^+ MLL-AF9 AML cells 40 days following secondary transplant (Figure S1L). Whereas 68% ± 15% or 25% ± 17% (mean ± SEM) of bone marrow (BM) cells were GFP^+ in mice transplanted with 10^4 or 2.5×10^3 control AML cells, respectively, only 0.06% ± 0.03% or 0.04% ± 0.03% of cells were GFP^+ in mice receiving *Kdm1a* KD cells. Together, these data demonstrate that *Kdm1a* is an essential regulator of murine MLL-AF9 LSCs and sustains the LSC potential of MLL AML cells through prevention of differentiation and apoptosis.

KDM1A Is Required to Sustain Expression of the MLL-AF9 Oncogenic Program

To investigate the genetic program regulated by KDM1A in murine MLL-AF9 AML cells enriched for LSCs (Somervaille and Cleary, 2006; Krivtsov et al., 2006), we compared the transcriptome of KIT^+Gr1^+ control and *Kdm1a* KD cells using exon arrays soon after initiation of KD (Figure 2A). Three separate samples from two different animals were used. At this time there was no immunophenotypic evidence of differentiation in *Kdm1a* KD cells (Figure 2A and data not shown).

Exonic expression values were condensed into gene level expression summaries (Table S2), which represent the mean expression value of the probe sets targeting the length of a given protein coding gene. *Kdm1a* was the most consistently and extensively downregulated gene in *Kdm1a* KD AML LSCs across the three sample pairs, as demonstrated by a signal-to-noise ranking metric (Figure 2B). In conventional comparative analyses, many more genes were downregulated than were

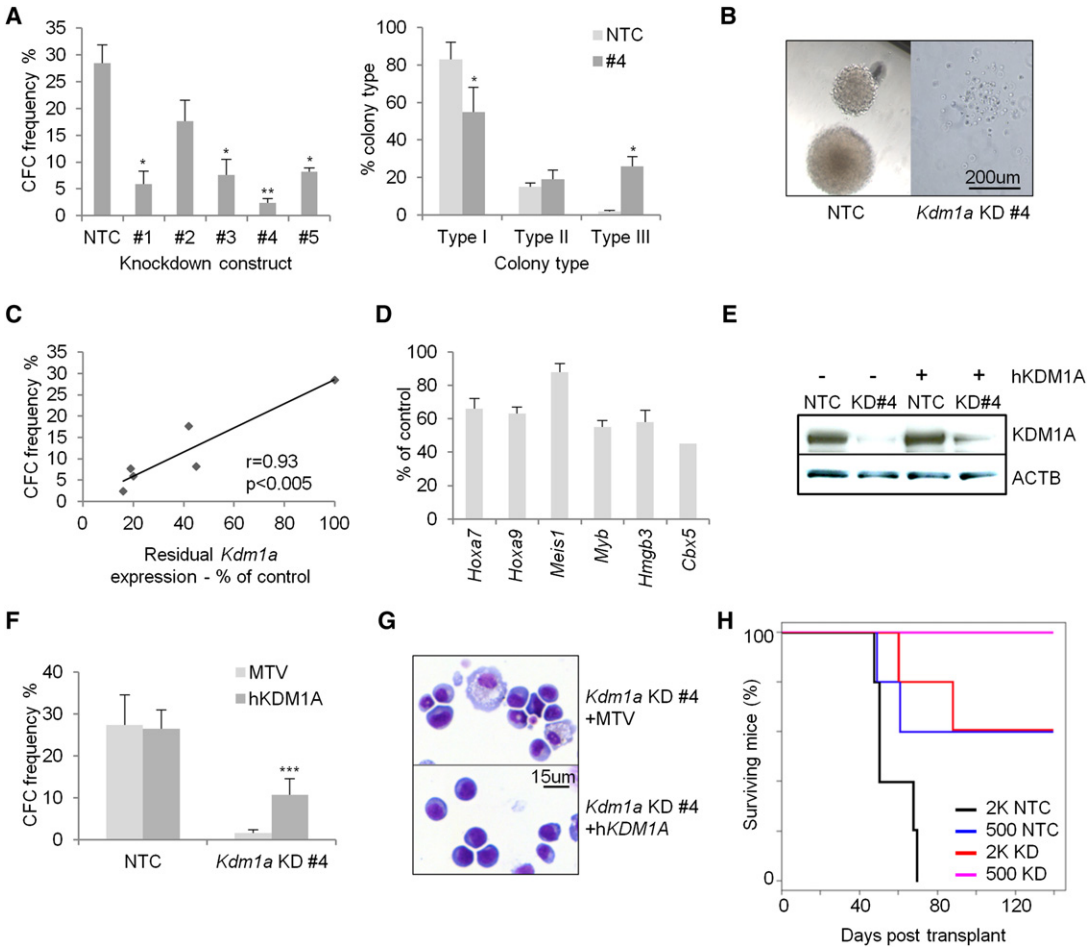

Figure 1. KDM1A Is an Essential Regulator of MLL-AF9 LSC

Murine MLL-AF9 AML BM cells were infected with lentiviruses expressing shRNAs targeting *Kdm1a* or a nontargeting control (NTC).

(A) Bar graphs show AML-CFC frequencies of control or *Kdm1a* KD cells (constructs #1–#5; left) or colony types formed by control (right) or *Kdm1a* KD (construct #4) cells, enumerated after six days of culture (mean ± SEM; n = 3; * indicates $p \leq 0.05$, ** indicates $p \leq 0.01$).

(B) Image shows typical type 1 or type 3 colonies.

(C) Graph shows correlation of *Kdm1a* KD with inhibition of CFC formation, as determined by qPCR 96 hr after KD initiation, for the five constructs tested.

(D) Relative expression of LSC-associated genes, as determined by qPCR, in *Kdm1a* KD cells (construct #4) compared with control cells after five days in semi-solid culture. Error bars refer to SEM of triplicate analyses.

(E) Western blot shows KDM1A expression in murine MLL-AF9 AML cells 48 hr following initiation of *Kdm1a* KD (construct #4) in the presence or absence of forced human KDM1A expression.

(F) Bar graph shows mean ± SEM AML-CFC frequencies of control and *Kdm1a* KD murine MLL-AF9 AML cells in the presence or absence of forced expression of human *KDM1A* (n = 8; *** indicates $p \leq 0.001$). MTV, empty pMSCV vector.

(G) Representative images of cytospin preparations of AML cells recovered at the end of semi-solid culture.

(H) Survival curves of sublethally irradiated syngeneic mice transplanted with 500 (n = 5) or 2,000 (n = 5) control or *Kdm1a* KD (construct #4) MLL-AF9 AML cells.

See also Figure S1 and Table S1.

upregulated (374 genes downregulated and 63 upregulated at $p \leq 0.05$ [paired t test] and 1.25-fold change; Figure 2C and Table S3). False discovery rates (1,000 permutations) were 12.0% and 76.2%, respectively, confirming the significance of the downregulated gene set. Genes consistently and significantly downregulated across the three sample pairs upon *Kdm1a* KD included leukemia-associated genes, such as *Ctnnb1* and *Id2*, and chromatin regulatory genes, such as Polycomb-regulatory complex 1 (PRC1) components *Bmi1*, *Pcgf1*, *Pcgf5*, and *Sfmbt1*; NuRD components *Mta3* and *Hdac2*; and ING2/HDAC complex components *Ing2*, *Arid4a*, and *Hdac2*. This initial analysis suggested that KDM1A contributes directly or indirectly to maintenance of expression of key transcription factors and chromatin regulatory genes in MLL-AF9 LSCs.

To identify gene sets whose co-ordinate expression was dependent upon KDM1A, we performed gene set enrichment analysis (GSEA; Subramanian et al., 2005). This revealed highly significant downregulation of gene sets required for, or associated with, MLL-AF9 leukemogenesis, including an MLL LSC-associated gene set (Somervaille et al., 2009; Figure 2D; NES −2.0; FDR 0%); the set of genes directly bound by MLL-AF9 in murine AML cells (Bernt et al., 2011; Figure 2E; NES −2.1;

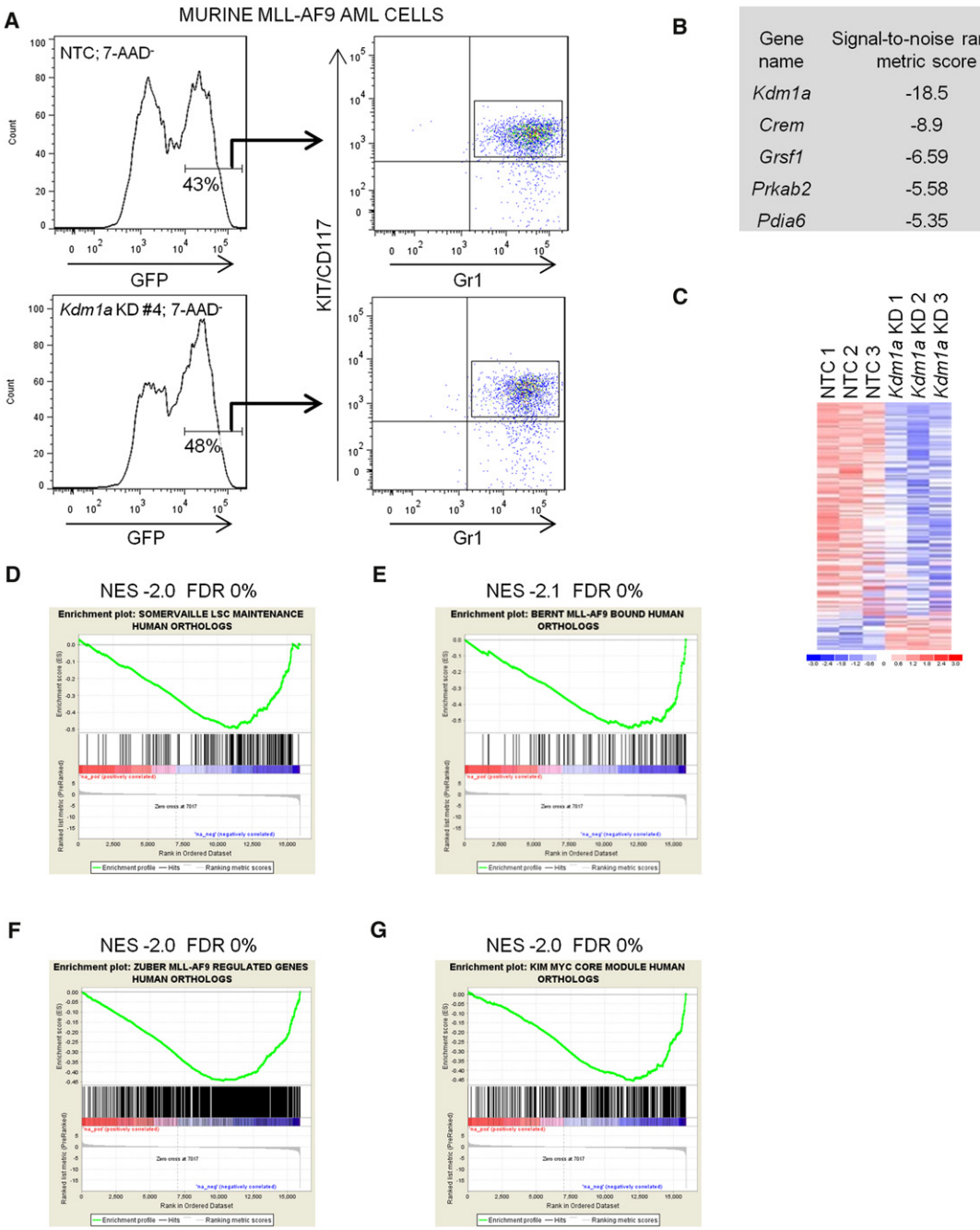

Figure 2. KDM1A Sustains Expression of an MLL-AF9-Associated Oncogenic Program

BM cells from mice with MLL-AF9 AML were infected with *Kdm1a* KD or nontargeting control lentiviruses, with GFP as a selectable marker.

(A) FACS plots show the gating strategy for sorting $GFP^+KIT^+Gr1^+$ control (NTC) or *Kdm1a* KD cells 42 hr following lentiviral infection.

(B) Table shows the five most consistently and extensively downregulated protein coding genes, according to a signal-to-noise ranking metric.

(C) Heat map represents 374 downregulated and 63 upregulated protein coding genes differentially expressed ($p \leq 0.05$; fold change ≥ 1.25) between *Kdm1a* KD and control samples (n = 3). Color scale indicates normalized expression values.

(D–G) GSEA plots show downregulation of (D) MLL LSC maintenance signature genes, (E) genes bound by MLL-AF9 in murine AML cells, (F) genes regulated by MLL-AF9 in murine MLL-AF9;$Nras^{G12D}$ AML cells, and (G) MYC "core module" genes in embryonic stem cells, in *Kdm1a* KD MLL-AF9 LSCs versus controls (for gene sets, see Table S5).

See also Tables S2–S6.

FDR 0%); the set of genes downregulated upon withdrawal of *MLL-AF9* expression in murine *MLL-AF9*;$Nras^{G12D}$ AML cells (Zuber et al., 2011a; Figure 2F; NES −2.0; FDR 0%) and MYC "core module" genes; the set of genes bound by the combination of MYC, MAX, MYCN, DMAP1, E2F1, E2F4, and ZFX in murine embryonic stem cells (ESCs; Kim et al., 2010; Figure 2G; NES

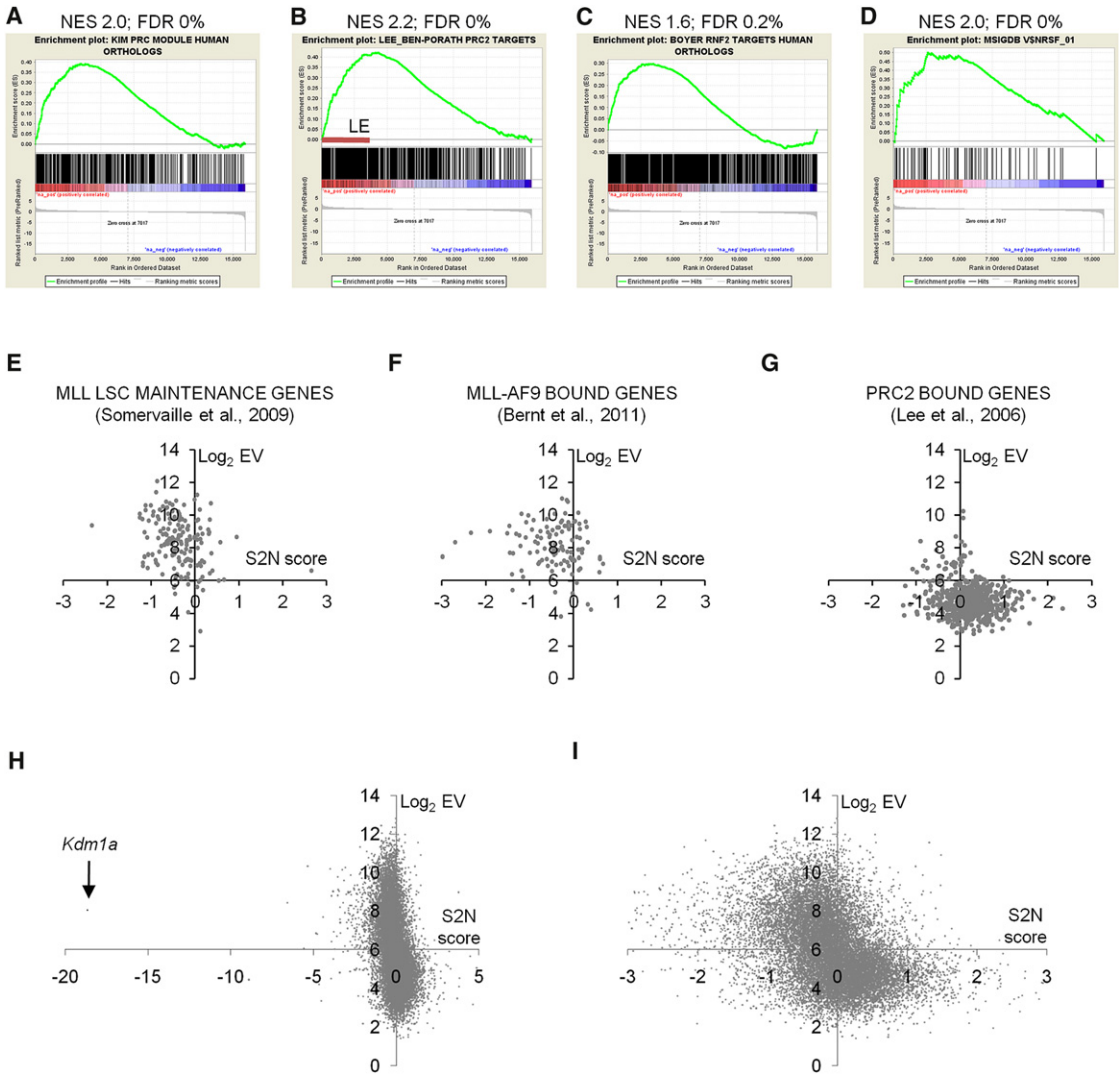

Figure 3. Derepression of Polycomb and REST Target Genes and Differential Regulation of Active versus Inactive Genes in *Kdm1a* KD MLL-AF9 AML cells

(A–D) GSEA plots show derepression of (A) Polycomb-related complex (PRC) module genes, (B) genes bound by PRC2 in ESCs, (C) genes bound by the PRC1 component RNF2 in ESCs, and (D) genes with a REST binding motif at their promoter in *Kdm1a* KD MLL-AF9 LSCs versus controls (for gene sets, see Table S5). LE, leading edge.

(E–G) Graphs show $\log_2$ gene level array expression values (Log_2 EV) versus signal-to-noise ranking metric scores (S2N score, reflecting change in expression; Table S4) for (E) MLL LSC maintenance signature genes, (F) genes bound by MLL-AF9, and (G) genes bound by PRC2 in ESCs. The x axis crosses at the median expression value for all protein coding genes.

(H and I) Graphs show Log_2 EV versus S2N score for (H) all 15,920 protein coding genes represented on the array that have annotated human orthologs or (I) those with S2N scores between −3 and 3.

−2.0; FDR 0%). These data show that KDM1A is required to sustain expression of oncogenic programs associated with MLL-AF9.

Derepression of Polycomb Targets following *Kdm1a* Knockdown

In contrast to simple comparative analysis, GSEA revealed coordinate upregulation of genes bound by Polycomb proteins in ESCs. In *Kdm1a* KD cells, there was significant enrichment in the set of upregulated genes of Polycomb-related complex (PRC) module genes (Figure 3A; NES 2.0; FDR 0%; Kim et al., 2010), which are genes co-occupied by SUZ12, EED, PHC1, and RNF2 in ESCs. Significant enrichment was also observed when genes targeted by PRC2 (Figure 3B; NES 2.2; FDR 0%; Lee et al., 2006; Ben-Porath et al., 2008; the set of genes co-occupied/marked by SUZ12, EED and H3K27Me3 in human ESCs) or the PRC1 component RNF2 (Figure 3C; NES 1.6; FDR 0.2%; Boyer et al., 2006) were considered separately. Many of the 279 genes in the PRC2 analysis "leading edge" (Figure 3B) were developmental regulators; 53 were annotated with the Swiss-Prot/Protein Information Resource keyword "Homeobox" ($p = 10^{-44}$), with roles in the development of skeletal muscle, nervous tissue, pancreas, heart, limbs, and sensory

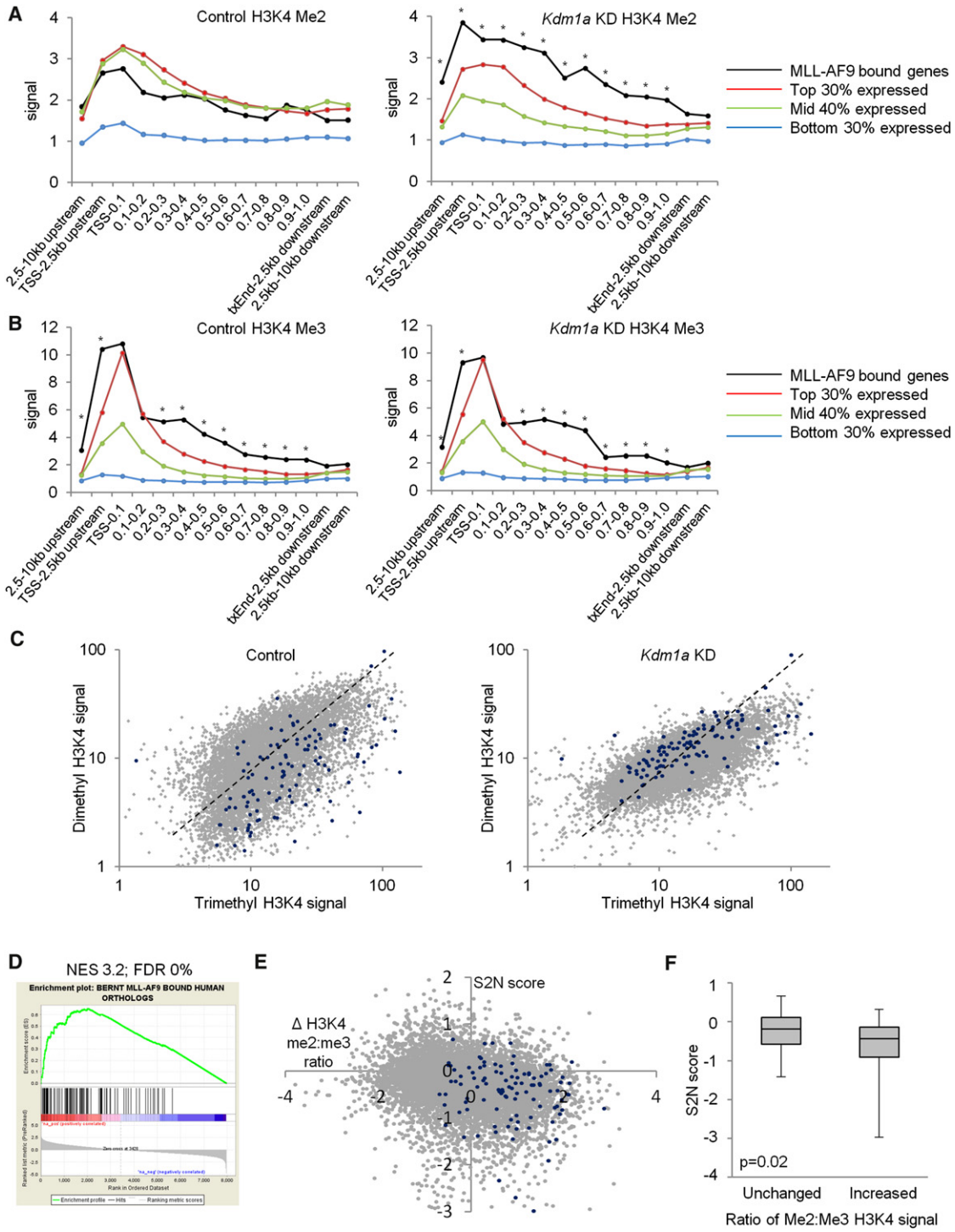

Figure 4. Selective Increase in Dimethyl-H3K4 ChIPseq Signal at MLL-AF9-Bound Genes in *Kdm1a* KD MLL-AF9 AML Cells

(A and B) *Kdm1a* KD or control murine MLL-AF9 AML cells were FACS purified 42 hr following lentiviral infection, with GFP as the selectable marker, and subjected to ChIPseq. Graphs show mean signal for (A) dimethyl-H3K4 and (B) trimethyl-H3K4 across and surrounding MLL-AF9 bound genes and non-MLL-AF9 bound genes with high, intermediate, and low level expression, in control (left panels) and KD cells (right panels). The open reading frame of each gene was divided into ten equal segments for the analysis. Signal is defined as mean uniquely mapped reads per kilobase per million reads. * indicates $p < 0.005$ for comparison of MLL-AF9 bound genes (black line) versus highly expressed non-MLL-AF9 bound genes (red line) at the same locus.

(C) Scatter plots show mean dimethyl- versus trimethyl-H3K4 signal for MLL-AF9 bound (blue dots) or non-MLL-AF9 bound (gray dots) genes with above median array expression values in control (left panel) or knockdown (right panel) cells. Dotted lines indicate median dimethyl:trimethyl H3K4 signal ratio for non-MLL-AF9 bound genes.

organs. There was also co-ordinate upregulation of genes with promoter regions containing a RE1-silencing transcription factor (REST)-binding motif (http://www.broadinstitute.org/gsea; Figure 3D; NES 2.1; FDR 0%). REST recruits KDM1A and RCOR1 (CoREST) to silence neuronal genes in nonneuronal tissues by demethylation of H3K4 (Lee et al., 2005). By contrast, there was no co-ordinate upregulation of genes associated with terminal myeloid differentiation, as demonstrated by GSEA using monocyte or neutrophil "fingerprint" gene sets or the set of genes upregulated during phorbol ester-induced macrophage differentiation of human THP1 MLL-AF9 AML cells (data not shown; for gene sets, see Table S5). Thus, while KDM1A contributes directly or indirectly to gene repression in MLL-AF9 AML LSCs, downregulation of the oncogenic program precedes upregulation of a myeloid differentiation program.

Differential Response of Active versus Less-Active/Repressed Genes

The above observations reflected more generalized, differential consequences for active versus less-active/repressed genes following *Kdm1a* KD. For example, MLL LSC maintenance signature genes (Somervaille et al., 2009) and genes bound by MLL-AF9 (Bernt et al., 2011), which were co-ordinately downregulated, almost exclusively exhibited above median array expression values (Figures 3E and 3F). By contrast, genes targeted by PRC2 in ESCs, which were co-ordinately upregulated, mostly exhibited below median expression levels (Figure 3G). Differential changes in expression of these discrete gene sets occurred in concert with a more generalized shift in gene expression, with downregulation of active genes (above median) and upregulation of less-active/repressed genes (below median; Figures 3H and 3I).

Selective Increase in Dimethyl-H3K4 ChIPseq Signal at MLL-AF9 Bound Genes following *Kdm1a* Knockdown

To investigate the effects of *Kdm1a* KD on histone modifications, we performed chromatin immunoprecipitation, followed by next-generation sequencing (ChIPseq), in control and *Kdm1a* KD MLL-AF9 AML cells for dimethyl-H3K4 and dimethyl-H3K9, as well as for trimethyl-H3K4 and trimethyl-H3K9. Dimethyl-H3K4 and dimethyl-H3K9 are targeted for demethylation by KDM1A. For each of these histone modifications, we compared the mean ChIPseq signal across and around protein-coding genes bound by the MLL-AF9 oncoprotein (Bernt et al., 2011; Table S5), with the mean signal from genes not bound by MLL-AF9 expressed at high, middle, or low levels (Table S2). As expected, in control cells the highest dimethyl- and trimethyl-H3K4 signal was observed surrounding promoter regions, with signal strength related to gene expression (Figures 4A, 4B, and S2A). Following *Kdm1a* KD, and consistent with localization of KDM1A in myeloid leukemia cells at active promoters and enhancers (Figure S2B; Ram et al., 2011), there was a highly significant increase in mean dimethyl-H3K4 signal at promoters and across bodies of genes bound by MLL-AF9 compared with other moderately or highly expressed non-MLL-AF9-bound genes (Figure 4A). By contrast, there was no significant increase in mean dimethyl-H3K4 signal when the MLL LSC-associated gene set (Somervaille et al., 2009), the set of genes downregulated upon withdrawal of *MLL-AF9* expression in murine *MLL-AF9;Nras*^{G12D} AML cells (Zuber et al., 2011a), or MYC "core module" genes (Kim et al., 2010) were considered (data not shown). Indeed, mean dimethyl-H3K4 signal decreased at moderately expressed non-MLL-AF9 bound genes (Figure 4A, green line). There was also no significant change in mean trimethyl-H3K4, dimethyl-H3K9, or trimethyl-H3K9 signal in *Kdm1a* KD versus control cells (Figures 4B, S2A–S2D), and there were only modest changes in global signals for each of the marks in western blotting analyses (Figure S2E). Thus, knockdown of the dimethyl-H3K4 demethylase KDM1A leads to a selective increase in dimethyl-H3K4 ChIPseq signal at genes bound by the MLL-AF9 oncoprotein.

The mean ratio of dimethyl-H3K4 to trimethyl-H3K4 signal was significantly lower in control cells at MLL-AF9-bound genes compared with non-MLL-AF9-bound genes expressed at above array median levels (0.54 ± 0.72 versus 0.88 ± 0.66, respectively [mean ± SD]; $p < 10^{-5}$; Figure 4C), due in large part to significantly greater trimethyl-H3K4 signal across the bodies of MLL-AF9-bound genes (Figure 4B). Following knockdown, ratios became comparable (0.84 ± 0.59 versus 0.76 ± 0.46, respectively [mean ± SD]; p = NS; Figure 4C). The significance of the selective increase in dimethyl-H3K4 signal at MLL-AF9-bound genes was further illustrated by GSEA (Figure 4D). MLL-AF9-bound genes cluster toward the top of a list of protein-coding genes ranked according to fold change in dimethyl-H3K4 marks in *Kdm1a* KD versus control cells (Table S7). Increased dimethyl:trimethyl H3K4 ratio at MLL-AF9-bound genes was associated with reduced expression (Figures 4E and 4F). Of note, we also observed a modest but significant excess of dimethyl- and trimethyl-H3K9 marks at MLL-AF9-bound genes by comparison with non-MLL-AF9-bound moderately or highly expressed genes (Figures S2C and S2D).

Together, these data are consistent with the concept of an epigenetic lesion in MLL leukemia (Guenther et al., 2008; Bernt et al., 2011) and suggest that, in this context, continued expression of MLL-AF9-bound genes may be directly dependent upon the colocalized dimethyl-H3K4 demethylase activity of KDM1A. The LSC maintenance or MYC module oncogenic programs, and other active genes, whose expression is subordinate to the set of MLL-AF9-bound genes, are likely indirectly dependent on KDM1A, downstream of MLL-AF9.

(D) GSEA plot shows enrichment of MLL-AF9-bound genes among protein coding genes ranked according to fold change in dimethyl-H3K4 ChIPseq signal in *Kdm1a* KD versus control cells (Table S7).
(E) Scatter plot shows $\log_2$ fold change in dimethyl:trimethyl H3K4 ratio (ΔH3K4 me2:me3 ratio) at MLL-AF9 bound (blue dots) and unbound (gray dots) genes in *Kdm1a* KD versus control cells plotted against their signal-to-noise metric (S2N) scores (reflecting change in expression; Table S4).
(F) Box plot shows median ± 25th percentile and range of S2N scores for MLL-AF9 bound genes with unchanged (i.e., −0.5 to 0.5) or increased (>1) $\log_2$ dimethyl:trimethyl H3K4 ratios.
See also Figure S2 and Table S7.

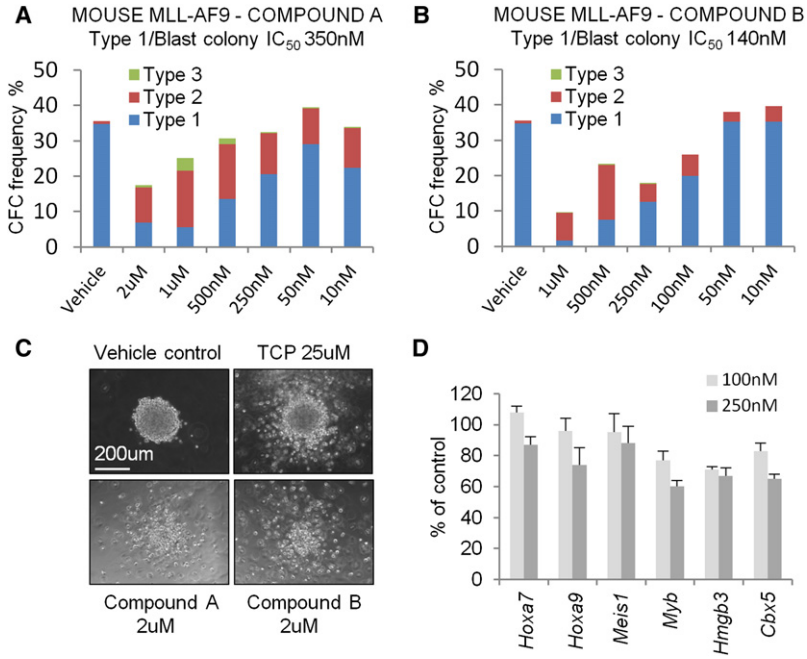

Figure 5. Tranylcypromine Analogs Phenocopy *Kdm1a* Knockdown

(A and B) Bar graphs show frequencies of colony types following treatment of AML cells with the indicated concentrations of Compounds A and B (means of three experiments and estimated biologic IC_{50} for type 1 colony formation are shown).

(C) Representative images of murine MLL-AF9 AML colonies after six days in semi-solid culture with the indicated type and concentration of inhibitor or vehicle.

(D) Relative expression of LSC-associated genes, as determined by qPCR, in murine MLL-AF9 AML cells treated with the indicated concentrations of Compound B compared with vehicle-treated cells after five days in semi-solid culture. Error bars refer to SEM of triplicate analyses.

See also Figure S3.

Pharmacologic Inhibition of KDM1A Phenocopies Knockdown in Murine and Primary Human MLL AML Cells

Given these data, *Kdm1a* represents an attractive therapeutic target in MLL leukemia. KDM1A is inhibited in vitro at an IC_{50} of ~20 μM by the monoamine oxidase inhibitor tranylcypromine (TCP) (Hou and Yu, 2010), which is used in the treatment of depression. We treated murine MLL-AF9 AML cells, human THP1 cells (which harbor a t(9;11) translocation, the cytogenetic hallmark of *MLL-AF9*), and primary human MLL leukemia cells with TCP. At a concentration close to the IC_{50} for KDM1A, TCP induced loss of clonogenic potential and induction of differentiation in murine (Figures S3A and S3B), human THP1 (Figures S3C and 3SD), and primary human MLL leukemic blasts (Figures S3E and S3F), as demonstrated by colony morphology and examination of cytospin preparations. Consistent with the depletion of type 1 myeloblast colonies by TCP treatment (Figure S3A) and our previous observation that MLL-AF9 AML-CFCs have LSC potential (Somervaille and Cleary, 2006), there was a significant delay in initiation of secondary AML by murine MLL-AF9 AML cells that had been incubated in vitro for five days with 25 μM TCP versus vehicle-treated control cells (Figure S3G).

In view of its lack of potency and selectivity, tranylcypromine is likely to be of limited use in the clinic. We therefore synthesized two analogs of tranylcypromine reported to be more potent and selective inhibitors of KDM1A (Guibourt, 2010): trans-N-((2,3-dihydrobenzo[b][1,4]dioxin-6-yl)methyl)-2-phenylcyclopropan-1-amine (hereafter Compound A) and trans-N-((2-methoxypyridin-3-yl)methyl)-2-phenylcyclopropan-1-amine (hereafter Compound B; Figure S3H). These compounds inhibited the enzymatic activity of KDM1A with IC_{50}s of 670 and 98 nM, respectively, versus 15.7 μM for tranylcypromine using the same assay (Figures S3I–3K). Treatment of murine MLL-AF9 AML cells with Compounds A and B phenocopied both *Kdm1a* KD and TCP treatment, also at concentrations close to their IC_{50}s for KDM1A (Figures 5A–5C; versus 8 μM for TCP; Figure S3A). Thus, the tested TCP analogs exhibited 23- and 57-fold greater biological potencies, respectively, than did TCP in a similar cell setting. As with *Kdm1a* KD, MLL-AF9 AML cells treated with Compound B also exhibited reduced expression of genes associated with LSC potential (Figure 5D), in particular core components of the LSC maintenance signature (Somervaille et al., 2009).

Next, we tested fresh cells from a patient newly diagnosed with high-count AML associated with a t(9;11) translocation, the hallmark of MLL-AF9 AML. As for murine MLL-AF9 cells, Compounds A and B inhibited colony formation of human MLL-AF9 AML cells and promoted differentiation in a dose-dependent manner (Figures 6A and 6B), with the effect being observed at biologic IC_{50}s of 270 and 50 nM, respectively. Following ten days of semi-solid culture, Compound B treatment induced both morphologic (Figure 6C) and immunophenotypic differentiation (Figures 6D and S4A–S4C), the latter demonstrated by reduction in the proportion of AML cells with an immature immunophenotype ($CD34^+CD14^-CD86^-CD36^-$). CD14, CD86, and CD36 are upregulated during monocyte/macrophage differentiation. A similar phenotype was observed following *Kdm1a* KD in primary AML cells from a patient with a t(6;11) translocation, the cytogenetic hallmark of *MLL-AF6* (Figures S4D and S4E). We also tested the effect of Compound B on the clonogenic potential in semi-solid culture of a panel of AML cell lines reflecting a range of molecular subtypes (Figure 6E). Whereas dose-dependent inhibition of colony formation was observed for most lines tested, the most striking inhibition was observed for MLL fusion oncogene-associated lines.

KDM1A Knockdown or Inhibition Spares the Clonogenic Potential of Normal Myeloid, but Not Erythroid, Progenitor Cells

Knockdown or inhibition of KDM1A in primary normal human $CD34^+$ hematopoietic cells significantly reduced the frequency of CFCs, predominantly due to loss of erythroid burst-forming units (BFU-E; Figures 7A–7E). The clonogenic potential of

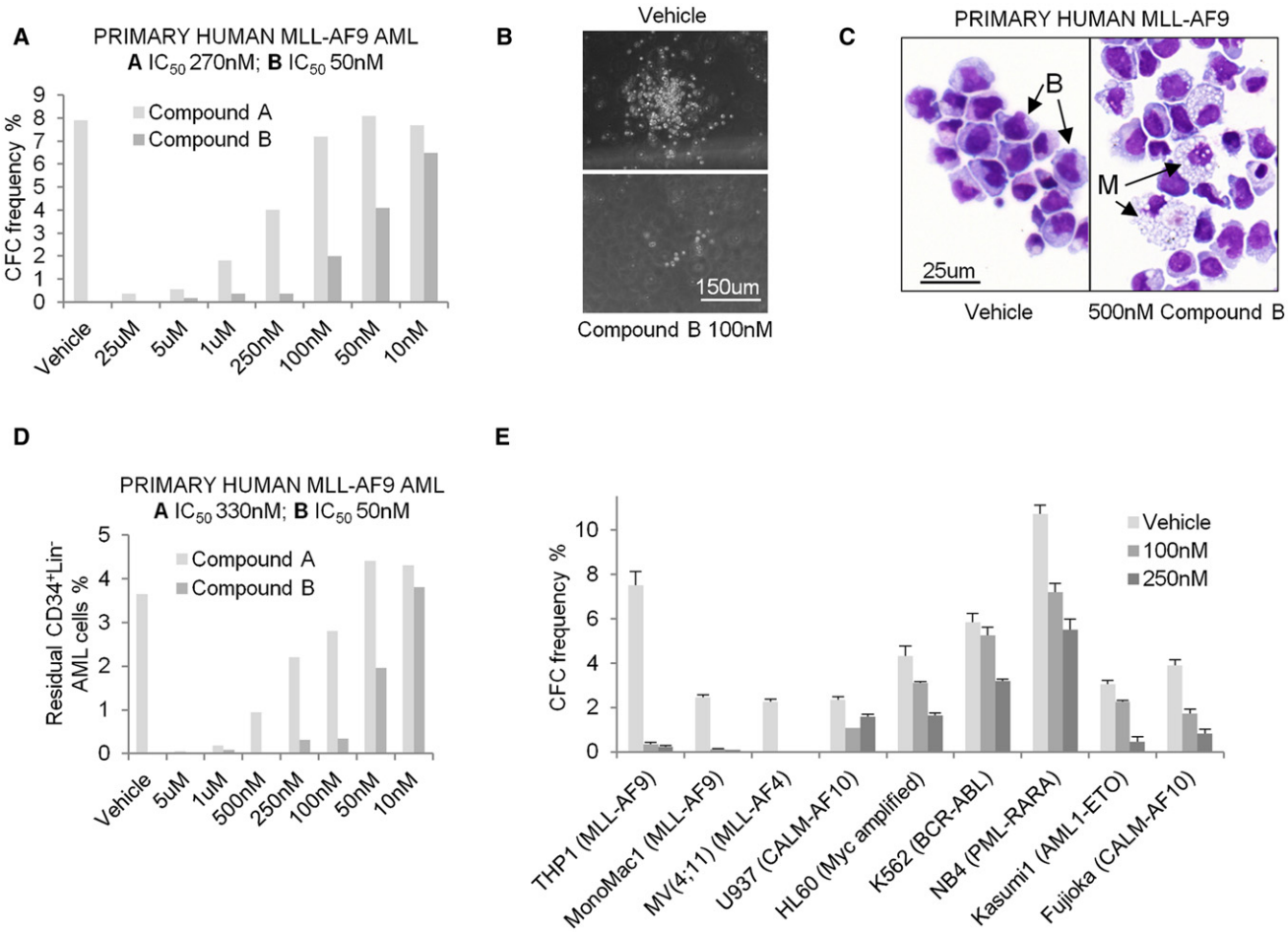

Figure 6. Tranylcypromine Analogs Phenocopy *Kdm1a* Knockdown in Human MLL Leukemia Cells

(A) Bar graph shows CFC frequencies of primary human MLL-AF9 AML cells after ten days in semi-solid culture with the indicated concentrations of Compounds A and B. Representative images show (B) primary human MLL-AF9 AML colonies (sample BB160) and (C) cytospin preparations of cells recovered at the end of semi-solid culture. B, blast; M, macrophage.

(D) Bar graph shows frequency of $CD34^+Lin^-$ ($CD14^-CD36^-CD86^-$) primary human MLL-AF9 AML cells at the end of semi-solid culture in the presence of the indicated concentration of KDM1A inhibitor, as determined by FACS analysis.

(E) Bar graph shows mean ± SEM CFC frequency in semi-solid culture of the indicated human AML cell lines following treatment with Compound B or vehicle (n = 3). See also Figure S4.

myeloid lineage colonies was preserved, although an increase in CFU-M was noted in Compound B-treated cells. For knockdown experiments, two different lentivirally expressed shRNAs, which reduced *KDM1A* expression to 31% (#1) or 38% (#2), respectively, were used. FACS analysis of TCP-treated $CD34^+$ cells after two weeks of culture revealed a significant reduction in the proportion of cells expressing high levels of glycophorin A (Figure 7F), a marker upregulated in the late stages of human erythroid differentiation. We found similar sparing of myeloid colony-forming potential in experiments using murine KIT^+ BM HSPCs cultured in conditions supporting myeloid development (data not shown).

Selective In Vivo Activity of KDM1A Inhibition versus MLL-AF9 Leukemia

To assess whether KDM1A inhibition also selectively targets MLL AML cells in vivo, we transplanted $CD45.2^+$ MLL-AF9 murine AML cells into sublethally irradiated $CD45.1^+$ congenic recipients and treated mice with DMSO vehicle, 10 mg/kg Compound B or 25 mg/kg Compound B twice daily by intraperitoneal injection according to the indicated schedule (Figure 8A). Plasma levels of Compound B measured one hour after a dose of 50 mg/kg IP were 2.0 ± 0.2 μM (n = 3), as determined by liquid chromatography-mass spectrometry. Complete blood counts and blood smears performed at the end of treatment in vehicle-treated mice demonstrated substantial leukemic leukocytosis with circulating blasts and leukemic myelomonocytic cells, modest anemia, and thrombocytopenia, consistent with incipient AML (Figures 8B and 8C). By contrast, mice treated with KDM1A inhibitor lacked evidence of circulating AML cells but were instead significantly more anemic and thrombocytopenic than were vehicle-treated controls and exhibited circulating nucleated erythroid precursors and polychromasia consistent with the degree of anemia (mean ± SEM hemoglobin

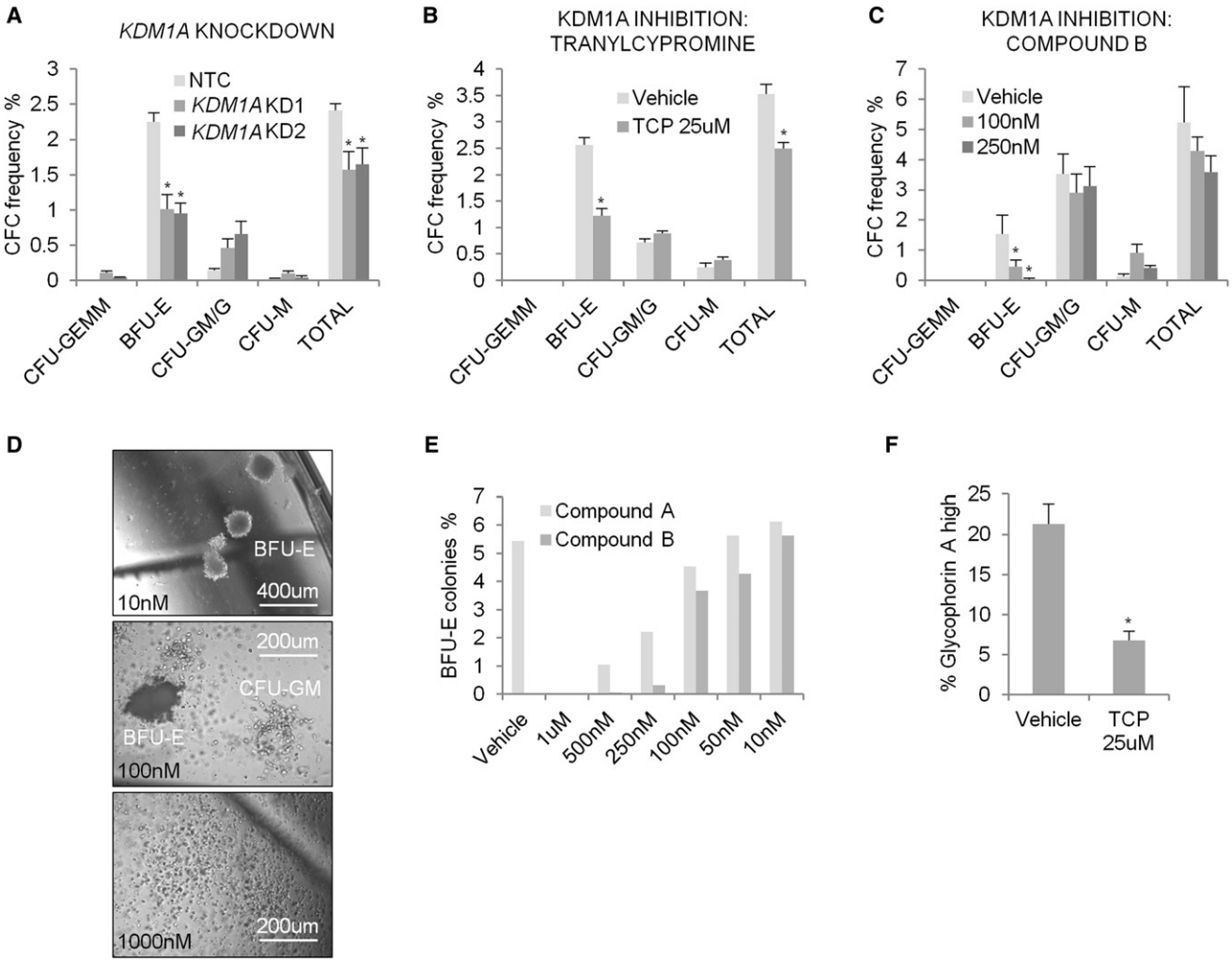

Figure 7. Preservation of Normal Myeloid, but Not Erythroid, Colonies following *KDM1A* Knockdown or Inhibition

(A and B) Bar graphs show CFC frequencies and colony types of normal human CD34$^+$ cells (A) infected with nontargeting control (NTC) or *KDM1A*-targeting (#1 and #2) lentiviruses, (B) treated with tranylcypromine 25 μM or (C) treated with the indicated concentrations of Compound B (mean ± SEM; n = 3; * indicates $p \leq 0.05$). Note sample-to-sample variability in BFU-E frequency in primary patient material.

(D) Representative images show colonies formed in the presence of the indicated concentrations of Compound B.

(E) Bar graph shows frequency of BFU-E arising from normal human CD34$^+$ HSPCs cultured in the indicated concentration of KDM1A inhibitor.

(F) Bar graph shows the percentage of glycophorin A$^+$ cells at the end of ten days in semi-solid culture of CD34$^+$ cells in the presence of tranylcypromine or vehicle (mean ± SEM; n = 3; * indicates $p \leq 0.05$). BFU-E, burst-forming unit erythroid; CFU-GM/G, colony-forming unit granulocyte/macrophage or colony-forming unit granulocyte; CFU-M, colony-forming unit macrophage.

5.0 ± 0.7 g/dl for mice receiving the 25 mg/kg dose vs. 9.0 ± 0.4 g/dl for vehicle-treated mice; $p < 0.001$; n = 6; mean ± SEM platelet count 89 ± 9 × 10^9/l for mice receiving the 25 mg/kg dose vs. 592 ± 55 × 10^9/l for vehicle-treated mice; $p < 0.001$; n = 6; Figures 8B and 8C). Thus, treatment of mice with KDM1A inhibitor completely blocked progression of MLL-AF9 leukemia into the circulation.

Consistent with this observation, analysis of AML cells aspirated from BM at the end of the treatment period showed a dose-dependent, significant reduction in both expression of KIT, which marks MLL-AF9 LSCs, and the frequency of AML-CFCs in FACS-purified CD45.2$^+$ AML cells (Figures 8D–8G). There was also a dose-dependent trend toward reduced donor:-recipient chimerism (Figure S5A). By contrast, neither KIT expression nor clonogenic potential of FACS-purified residual CD45.1$^+$ normal hematopoietic cells were impacted by treatment with KDM1A inhibitor (Figures 8E and 8H). Furthermore, FACS-purified CD45.1$^+$KIT$^+$Gr1$^-$ normal cells from KDM1A inhibitor-treated mice retained lympho-myeloid repopulating activity in secondary transplantation assays (Figures 8I–8K). Although there was a trend toward prolonged survival for leukemic mice treated with Compound B (Figure S5B), a number of mice died of drug-induced anemia rather than leukemia, thus confounding interpretation of survival as an endpoint. Finally, we treated immune-deficient mice xenografted with primary human MLL-AF6 AML cells with Compound B. By comparison, with vehicle-treated mice, a higher proportion of human AML cells in animals treated with KDM1A inhibitor expressed the

monocyte/macrophage differentiation markers CD36 and CD86, and fewer cells expressed an immature $CD34^{+}CD36^{-}CD86^{-}$ immunophenotype (Figure S5C).

Together, these in vitro and in vivo data demonstrate that different types of normal and malignant hematopoietic cells exhibit differential sensitivities to pharmacologic KDM1A inhibition. The relative sensitivity of MLL-AF9 AML cells by comparison with normal HSPCs suggests a significant therapeutic window.

Discussion

Our genetic and pharmacologic data using murine models and primary human AML cells demonstrate that KDM1A is required to sustain the expression of the MLL-AF9-associated oncogenic program, thus maintaining the oncogenic potential of MLL-AF9 LSCs. They also highlight the enzyme as a potential therapeutic target in MLL leukemias, which is of importance given the development of KDM1A inhibitors by the pharmaceutical industry (Guibourt, 2010). The progeny of individually isolated blast-like (type 1) MLL-AF9 AML colonies (Figure 1B) reliably initiate AML in secondarily transplanted recipients, demonstrating the identity of the parental CFC as a cell with LSC potential (Somervaille and Cleary, 2006). Thus, our observation that *Kdm1a* KD or inhibition resulted in loss of AML-CFCs, with induction of differentiation, was highly significant, as was the observation that *Kdm1a* KD MLL-AF9 AML cells fail to initiate leukemia in secondary transplantation experiments. Although a direct link between in vitro clonogenic potential and LSC potential in primary human MLL AML has not been proven, it is nevertheless of note that we found frequencies of clonogenic cells in patient samples ranging from 1%–9%, not dissimilar to those found in the murine model.

KDM1A Sustains Expression of the MLL-AF9 Oncogenic Program

Recent studies have associated the expression of defined gene sets with the oncogenic potential of MLL LSCs (Somervaille et al., 2009; Kim et al., 2010; Bernt et al., 2011; Zuber et al., 2011a). At an early time point following initiation of *Kdm1a* KD in murine MLL-AF9 LSCs, these gene sets were co-ordinately downregulated, and this occurred prior to upregulation of gene sets or cell surface markers associated with terminal myeloid differentiation or the onset of apoptosis in some cells. Loss of clonogenic potential with induction of differentiation and apoptosis is a phenotype very similar to that observed upon tamoxifen withdrawal from murine BM HSPCs immortalized by an MLL-ENL estrogen receptor fusion (Somervaille et al., 2009). This observation suggests the possibility that KDM1A might have a close physical or functional interaction with MLL-AF9, acting as an essential oncogenic cofactor to maintain transformation.

Two lines of evidence suggest this may be the case. First, KDM1A is a member of an ELL complex identified in 293 cells (Biswas et al., 2011), which includes pTEFb members CDK9 and CCNT1 and the MLL oncogenic fusion partners AFF1 (also known as AF4) and AFF4 (also known as AF5q). ELL, CDK9, CCNT1, AFF1, and AFF4 associate with one another either in a static "super-elongation complex" (SEC) or in a dynamic set of higher order complexes that interact with MLL oncogenic fusions, including MLL-AF9 (Lin et al., 2010; Yokoyama et al., 2010). Such interactions may serve to recruit KDM1A to genomic loci bound by MLL oncoproteins. The second piece of evidence arises from our ChIP-sequencing analyses, which suggest a "footprint" of KDM1A activity at genomic loci bound by MLL-AF9. While KDM1A binds promiscuously across the genome, especially at active promoters and enhancers (Ram et al., 2011), following *Kdm1a* KD we observed a highly significant and selective increase in dimethyl-H3K4 ChIPseq signal at genes bound by the MLL-AF9 oncoprotein (Bernt et al., 2011), which was associated with co-ordinate downregulation of the same gene set. Dimethyl-H3K4 is a demethylation target for KDM1A. Of note, global changes in ChIPseq signals were only observed for the dimethyl-H3K4 mark; a global change in the pattern of histone modifications at the gene sets analyzed was not observed for the other marks investigated, including dimethyl-H3K9, which is also a demethylation target of KDM1A. Thus, the only histone modification that exhibited significant change at MLL-AF9-bound genes following *Kdm1a* KD is an enzymatic target of KDM1A.

This observation was unexpected because the dimethyl-H3K4 mark has been considered to be associated with active transcription and its removal by KDM1A has been considered to be associated with transcription repression. Examples of the repressive function of KDM1A include its recruitment with RCOR1 (CoREST) by REST to silence neuronal genes in non-neuronal cells (Lee et al., 2005), its recruitment by ZEB1 to the *Gh* promoter to suppress *Gh* expression in pituitary lactotrophs (Wang et al., 2007), and its recruitment by GFI1 (Saleque et al., 2007) or TAL1 (Hu et al., 2009) to their respective target genes in early erythroid development. KDM1A is also an established transcription activator, although in the context of demethylation of the repression-associated dimethyl-H3K9 mark. For example, it demethylates dimethyl-H3K9 to facilitate androgen- or estrogen-dependent transcription in prostate or breast cancer cells, respectively, by opposing the activity of H3K9 methyltransferases (Metzger et al., 2005; Garcia-Bassets et al., 2007). Likewise, in development, KDM1A is required for activation of *Gh* transcription in pituitary precursor cells (Wang et al., 2007). Our observations in MLL-AF9 AML cells suggest a role for KDM1A in the context of the epigenetic lesion associated with MLL leukemia. This lesion is characterized by an abnormal extent and distribution of the elongation-associated dimethyl-H3K79 mark and the transcription initiation-associated trimethyl-H3K4 mark at genes bound by MLL oncoproteins, as well as mistargeting of elongation factors, such as MLLT1 (also known as ENL; Guenther et al., 2008; Bernt et al., 2011). In keeping with Guenther et al. (2008), we also observed an excess of trimethyl-H3K4 marks upstream of the promoter and across the bodies of genes bound by MLL-AF9.

It was of note that in control MLL-AF9 AML cells the ratio of dimethyl:trimethyl H3K4 marks at MLL-AF9-bound genes was significantly lower than that of non-MLL-AF9-bound genes expressed at similar levels, in large part due to comparatively higher levels of trimethyl-H3K4. Ratios became similar following *Kdm1a* KD. Our data are consistent with a model in which KDM1A acts at MLL-AF9-bound genes to maintain low levels of dimethyl- relative to trimethyl-H3K4, a chromatin state presumably permissive for levels of transcription required for oncogenic transformation. This raises the question as to how

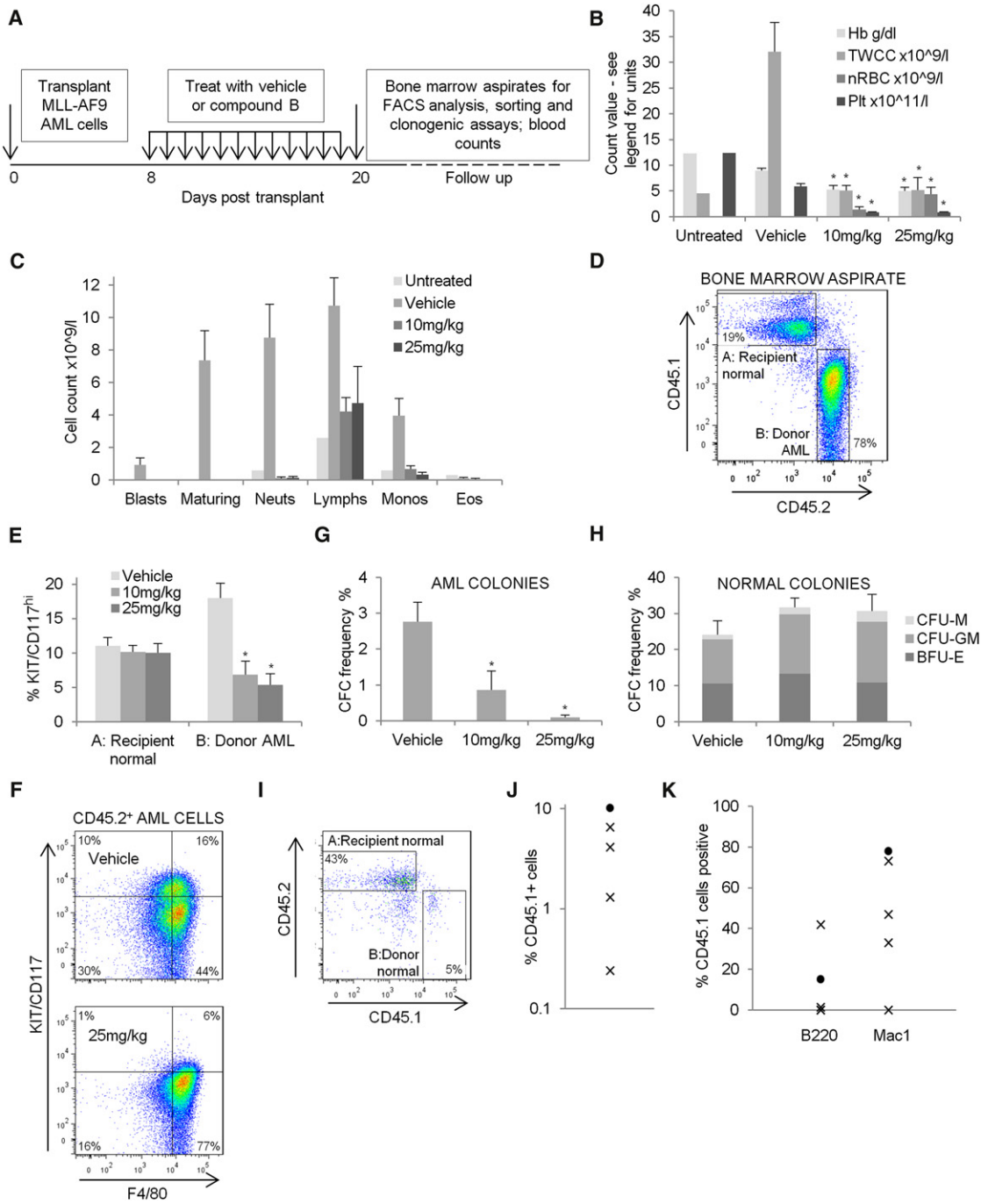

Figure 8. Selective In Vivo Efficacy of KDM1A Inhibition versus MLL-AF9 AML Cells

(A) Image shows experimental plan.

(B) Bar chart shows mean ± SEM hemoglobin (Hb), total white cell count (TWCC), nucleated red blood cell count (nRBC), and platelet count (Plt) in complete blood counts from mice after 12 days of treatment with DMSO vehicle or Compound B at the indicated dose (n = 6 for each cohort). * indicates $p < 0.01$ for values from KDM1A inhibitor-treated mice compared with vehicle-treated controls. Blood count values from an untreated normal adult C57BL/6 mouse are shown for comparison.

(C) Bar chart shows mean ± SEM leukocyte manual differential counts in blood smears from vehicle- and KDM1A inhibitor-treated mice (n = 6 for each cohort). Values from an untreated normal adult C57BL/6 mouse are shown for comparison. Maturing, maturing leukemic myelomonocytic cells; Neuts, neutrophils, including leukemic neutrophils; Lymphs, lymphocytes; Monos, monocytes; Eos, eosinophils.

(D) Representative FACS plot shows chimerism of $CD45.1^+$ normal recipient hematopoietic cells (A, Recipient normal) and $CD45.2^+$ AML cells (B, Donor AML) in a BM aspirate sample taken on day 20 post-transplant.

(E) Bar graph shows mean ± SEM percentage of $CD45.1^+$ normal recipient or $CD45.2^+$ AML cells co-expressing KIT. * indicates $p < 0.01$ for comparison of vehicle-treated versus Compound B-treated mice (n = 6).

accumulation of dimethyl-H3K4 marks might be inhibitory. It is clear from work in yeast that dimethyl-H3K4 is a functionally distinct modification and not simply a metabolic intermediate between monomethyl- and trimethyl-H3K4. It serves as a platform for recruitment of a Set3 complex that contains histone deacetylase activity, which reduces acetylation toward the 5′ end of genes to suppress transcription from cryptic internal promoters (Kim and Buratowski, 2009). Furthermore, chromatin state maps of the genome indicate that increased ratios of dimethyl:trimethyl H3K4 are observed at poised or weakly active promoters by comparison with fully activated promoters (Ernst et al., 2011). Thus, accumulation of dimethyl-H3K4 marks at MLL oncoprotein-bound genes may enable locoregional binding of complexes that repress transcription, leading to downregulation of genes bound by MLL-AF9. Reduced expression of other actively expressed genes, including subordinate oncogenic programs, such as the LSC maintenance program and MYC module, and increased expression of Polycomb-bound genes, is likely an indirect effect of *Kdm1a* KD, downstream of the set of genes bound by MLL-AF9, because we did not observe coordinate changes in histone methylation status at these genomic loci. With regard to Polycomb bound genes, for example, among those most highly downregulated upon *Kdm1a* KD were genes coding for components of PRC1, including *Bmi1*, which is required for stable maintenance of transcriptionally repressed states.

KDM1A as a Therapeutic Target in Leukemia

KDM1A has been suggested as a therapeutic target in cancer because of its high-level expression in poor-risk prostate adenocarcinoma (Kahl et al., 2006), poorly differentiated neuroblastoma (Schulte et al., 2009), and high-grade ER-negative breast cancer (Lim et al., 2010). Our data suggest a therapeutic role for KDM1A inhibition in leukemias associated with expression of MLL fusion oncoproteins. This is demonstrated by the use of potent KDM1A inhibitors selectively to induce loss of clonogenic potential and induction of differentiation in both murine and primary human MLL leukemia cells, both in vitro and in vivo. KDM1A inhibitor treatment of mice engrafted with congenic MLL-AF9 AML cells prevented progression of AML cells into the circulation, downregulated expression of the LSC marker KIT, and reduced the frequency of AML cells with clonogenic potential. Similarly, it also induced immunophenotypic differentiation of xenografted primary human MLL-AF6 cells. By contrast, normal HSPCs were spared as demonstrated by unchanged expression of KIT, unchanged clonogenic potential in semi-solid culture, and a retained capacity to provide lympho-myeloid reconstitution in secondary transplant experiments. KDM1A inhibition in congenic transplant recipients also resulted in a trend toward prolonged survival, although survival curves were confounded by treated mice dying as a result of drug-induced anemia. The effect of KDM1A inhibition on erythropoiesis was predicted by our in vitro studies, which showed a selective loss of BFU-E activity in normal human $CD34^+$ cells following both *Kdm1a* KD and inhibition. Together, these data point to a significant potential therapeutic window for the use of KDM1A inhibitors in the MLL molecular subtype of AML.

Such differential consequences for different normal and malignant hematopoietic cell types are consistent with a previous study using murine cell lines; *Kdm1a* KD impaired DMSO-induced erythroid differentiation of MEL cells and phorbol ester-induced megakaryocytic differentiation of L8057 cells but induced granulocytic differentiation of 32D.4 cells (Saleque et al., 2007). Thus, KDM1A depletion or inhibition has differing consequences for different cellular subtypes.

How might KDM1A inhibitors be used therapeutically? Induction of differentiation of leukemic blasts using all-trans retinoic acid (ATRA) is standard therapy in one subtype of AML, acute promyelocytic leukemia (APML). However, whereas ATRA alone may induce remission, it is insufficient for cure and concomitant treatment with anthracyline or arsenic trioxide is required (Sanz and Lo-Coco, 2011). Indeed single-agent therapy in AML is rarely, if ever, curative. One option may be the combination of KDM1A inhibition with chemotherapy, as has been historically effective for APML and ATRA. Alternatives might include single agent maintenance therapy or combination therapy with histone deacetylase (HDAC) inhibitors, because KDM1A inhibition sensitizes breast cancer and glioblastoma cells to HDAC inhibitor-induced cell cycle arrest or apoptosis (Singh et al., 2011; Huang et al., 2012). Anemia or thrombocytopenia associated with therapy could be managed by transfusion. KDM1A inhibitors may be also of value in certain myeloproliferative disorders.

Examination of a web-based repository of microarray data from primary human AML samples (http://www.oncomine.org) shows that *KDM1A* is expressed at comparable levels in MLL-rearranged leukemias to those in other molecular subtypes. Although our human cell line data suggest that MLL oncoprotein leukemias are selectively sensitive to KDM1A inhibition by comparison with other molecular subtypes of AML, dose-dependent inhibition of clonogenic potential was also observed for other lines, for example, NB4 cells and Kasumi1 cells (associated with *PML-RARA* and *RUNX1-RUNX1T1*, respectively). This suggests the possibility that KDM1A inhibition

(F) Representative FACS plots show expression of KIT and the monocyte/macrophage differentiation marker F4/80 in AML cells in BM aspirates from mice treated with the vehicle (upper panel) or 25 mg/kg Compound B (lower panel).
(G) Bar graph shows mean ± SEM AML-CFC frequency in $CD45.2^+$ MLL-AF9 AML cells, as determined by semi-solid culture.
(H) Bar graph shows mean ± SEM CFC frequency, and colony type, in normal $CD45.1^+$ cells FACS purified from BM aspirates, as determined by semi-solid culture (for G and H, * indicates $p < 0.01$ for comparison of vehicle-treated versus Compound B-treated mice [n = 6]). BFU-E, burst-forming unit erythroid; CFU-GM, colony-forming unit granulocyte/macrophage; CFU-M, colony-forming unit macrophage.
(I) FACS plot shows donor:recipient chimerism in a BM aspirate 21 days following transplantation of 1,000 normal $CD45.1^+KIT^+Gr1^+$ cells, FACS purified from mice treated with Compound B, into a sublethally irradiated normal $CD45.2^+$ congenic recipient.
(J) Graph shows percentage donor ($CD45.1^+$) chimerism in BM aspirates for each of the five recipients transplanted with 1,000 cells (x indicates cells were from mice receiving a 25mg/kg dose; ● indicates cells were from mice receiving a 10 mg/kg dose).
(K) Graph indicates percentage of donor engrafted cells positive for B-lineage (B220) or myeloid lineage (Mac1) markers.
See also Figure S5.

may be a useful therapeutic strategy in other types of myeloid malignancy. Consistent with this, *KDM1A* is among the 5% most highly expressed genes in microarray data sets from prospectively purified immunophenotypic LSCs from a variety of distinct AML subtypes (data extracted from Goardon et al., 2011).

In summary, our identification of KDM1A as a candidate therapeutic target in the MLL translocated subtype of AML adds to recent studies suggesting new approaches to treat this disease, including inhibition of the DOT1L H3K79 histone methyltransferase (Bernt et al., 2011) and the bromodomain protein BRD4 (Zuber et al., 2011b; Dawson et al., 2011). Our data mandate further studies of the effects of KDM1A inhibition in other subtypes of myeloid malignancy, evaluation of combination therapies and clinical trials in AML of KDM1A inhibitors in development by the pharmaceutical industry.

EXPERIMENTAL PROCEDURES

Vectors, Reagents, Cell Lines, Chemicals, and Antibodies

Details of retroviral and lentiviral vectors, cell lines, chemicals, FACS, western blotting, or chromatin immunoprecipitation antibodies are in the Supplemental Experimental Procedures. Tranylcypromine analogs trans-N-[1-(2,3-dihydro-1,4-benzodioxin-6-yl)ethyl]-2-phenylcyclopropan-1-amine (Compound A) and trans-N-[(2-methoxypyridin-3-yl)methyl]-2-phenylcyclopropan-1-amine (Compound B) were synthesized in house, as described in Guibourt (2010).

Chromatin Immunoprecipitation and Next-Generation Sequencing

Chromatin immunoprecipitation (ChIP) was performed using a Red ChIP Kit (Diagenode, Liege, Belgium) in accordance with the manufacturer's instructions. Details of shearing, ChIPseq library preparation, next-generation sequencing, and bioinformatics analysis are in the Supplemental Experimental Procedures. ChIPseq BED files and raw data files are available at http://www.ncbi.nlm.nih.gov/geo/ under the accession number GSE36348.

Flow Cytometry

FACS analyses were performed using an LSR Model II flow cytometer (BD Biosciences, Oxford, UK). Cell sorting experiments were performed using either an Influx or a FACS Aria flow cytometer (both from BD Biosciences).

Mice and Murine Experiments

Experiments were approved by the Paterson Institute's Animal Ethics Committee and performed under a project license issued by the United Kingdom Home Office, in keeping with the Home Office Animal Scientific Procedures Act, 1986. C57BL/6 ($CD45.2^+$) mice were purchased from Harlan (Shardlow, UK). B6.SJL-*Ptprc*^{a} *Pepc*^{b}/BoyJ ($CD45.1^+$) and NOD.Cg-*Prkdc*^{scid} *Il2rg*^{tm1Wjl}/SzJ mice were purchased from Jackson Laboratories (Bar Harbor, ME, USA) and bred in house. Details of experimental initiation of murine MLL-AF9 leukemia (both primary and secondary), lentiviral infection of cryopreserved AML cells, and clonogenic assays of normal and leukemic cells are in the Supplemental Experimental Procedures.

Human Tissue and Experiments

Use of human tissue was in compliance with the ethical and legal framework of the Human Tissue Act, 2004. Normal human $CD34^+$ mobilized HSPCs surplus to requirements were from patients undergoing chemotherapy and autologous transplantation for lymphoma and myeloma. Their use was authorized by the Salford and Trafford Research Ethics Committee and, where possible, following the written informed consent of donors. Primary human AML blasts were from Manchester Cancer Research Centre's Tissue Biobank (instituted with approval of the South Manchester Research Ethics Committee); their use was authorized following ethical review by the Tissue Biobank's scientific sub-committee. Written informed consent was obtained for all samples donated to the Biobank. Details of lentiviral infection protocols and clonogenic assays are in the Supplemental Experimental Procedures.

RNA Extraction, Quantitative PCR, Microarray Hybridization, and Data Analysis

Details are in the Supplemental Experimental Procedures. Exon array CEL files are available at http://www.ncbi.nlm.nih.gov/geo/ under the accession number GSE36348.

SUPPLEMENTAL INFORMATION

Supplemental Information includes five figures, Supplemental Experimental Procedures, and seven tables and can be found with this article online at doi:10.1016/j.ccr.2012.03.014.

ACKNOWLEDGMENTS

We thank Mark Wappett, Morgan Blaylock, Jeff Barry, Michael Hughes, Helen Small, Gail Bruder, Angela Cleworth, Angela Cooke, Yvonne Hey, Stuart Pepper, Jodie Whitaker, and Gillian Newton for technical support, as well as Nullin Divecha, Valerie Kouskoff, and Georges Lacaud for a critical reading of the manuscript. This work was supported by Cancer Research UK (grant numbers C480/A12328 and C480/A11411). B.F.G. was supported by a Leukaemia and Lymphoma Research Clinical Training Fellowship.

Received: October 24, 2011
Revised: January 30, 2012
Accepted: March 8, 2012
Published online: March 29, 2012

REFERENCES

Ben-Porath, I., Thomson, M.W., Carey, V.J., Ge, R., Bell, G.W., Regev, A., and Weinberg, R.A. (2008). An embryonic stem cell-like gene expression signature in poorly differentiated aggressive human tumors. Nat. Genet. *40*, 499–507.

Bernt, K.M., Zhu, N., Sinha, A.U., Vempati, S., Faber, J., Krivtsov, A.V., Feng, Z., Punt, N., Daigle, A., Bullinger, L., et al. (2011). MLL-rearranged leukemia is dependent on aberrant H3K79 methylation by DOT1L. Cancer Cell *20*, 66–78.

Biswas, D., Milne, T.A., Basrur, V., Kim, J., Elenitoba-Johnson, K.S., Allis, C.D., and Roeder, R.G. (2011). Function of leukemogenic mixed lineage leukemia 1 (MLL) fusion proteins through distinct partner protein complexes. Proc. Natl. Acad. Sci. USA *108*, 15751–15756.

Boyer, L.A., Plath, K., Zeitlinger, J., Brambrink, T., Medeiros, L.A., Lee, T.I., Levine, S.S., Wernig, M., Tajonar, A., Ray, M.K., et al. (2006). Polycomb complexes repress developmental regulators in murine embryonic stem cells. Nature *441*, 349–353.

Dawson, M.A., Prinjha, R.K., Dittmann, A., Giotopoulos, G., Bantscheff, M., Chan, W.I., Robson, S.C., Chung, C.W., Hopf, C., Savitski, M.M., et al. (2011). Inhibition of BET recruitment to chromatin as an effective treatment for MLL-fusion leukaemia. Nature *478*, 529–533.

Ernst, J., Kheradpour, P., Mikkelsen, T.S., Shoresh, N., Ward, L.D., Epstein, C.B., Zhang, X., Wang, L., Issner, R., Coyne, M., et al. (2011). Mapping and analysis of chromatin state dynamics in nine human cell types. Nature *473*, 43–49.

Fathi, A.T., and Abdel-Wahab, O. (2012). Mutations in epigenetic modifiers in myeloid malignancies and the prospect of novel epigenetic-targeted therapy. Adv. Hematol. *2012*, 469592.

Fenaux, P., Mufti, G.J., Hellstrom-Lindberg, E., Santini, V., Finelli, C., Giagounidis, A., Schoch, R., Gattermann, N., Sanz, G., List, A., et al; International Vidaza High-Risk MDS Survival Study Group. (2009). Efficacy of azacitidine compared with that of conventional care regimens in the treatment of higher-risk myelodysplastic syndromes: a randomised, open-label, phase III study. Lancet Oncol. *10*, 223–232.

Garcia-Bassets, I., Kwon, Y.S., Telese, F., Prefontaine, G.G., Hutt, K.R., Cheng, C.S., Ju, B.G., Ohgi, K.A., Wang, J., Escoubet-Lozach, L., et al. (2007). Histone methylation-dependent mechanisms impose ligand dependency for gene activation by nuclear receptors. Cell *128*, 505–518.

Goardon, N., Marchi, E., Atzberger, A., Quek, L., Schuh, A., Soneji, S., Woll, P., Mead, A., Alford, K.A., Rout, R., et al. (2011). Coexistence of LMPP-like and

GMP-like leukemia stem cells in acute myeloid leukemia. Cancer Cell *19*, 138–152.

Guenther, M.G., Lawton, L.N., Rozovskaia, T., Frampton, G.M., Levine, S.S., Volkert, T.L., Croce, C.M., Nakamura, T., Canaani, E., and Young, R.A. (2008). Aberrant chromatin at genes encoding stem cell regulators in human mixed-lineage leukemia. Genes Dev. *22*, 3403–3408.

Guibourt, N. July 2010. Phenylcyclopropylamine derivatives and their medical use. International Patent, WO2010/084160.

Hou, H., and Yu, H. (2010). Structural insights into histone lysine demethylation. Curr. Opin. Struct. Biol. *20*, 739–748.

Hu, X., Li, X., Valverde, K., Fu, X., Noguchi, C., Qiu, Y., and Huang, S. (2009). LSD1-mediated epigenetic modification is required for TAL1 function and hematopoiesis. Proc. Natl. Acad. Sci. USA *106*, 10141–10146.

Huang, Y., Vasilatos, S.N., Boric, L., Shaw, P.G., and Davidson, N.E. (2012). Inhibitors of histone demethylation and histone deacetylation cooperate in regulating gene expression and inhibiting growth in human breast cancer cells. Breast Cancer Res. Treat. *131*, 777–789.

Kahl, P., Gullotti, L., Heukamp, L.C., Wolf, S., Friedrichs, N., Vorreuther, R., Solleder, G., Bastian, P.J., Ellinger, J., Metzger, E., et al. (2006). Androgen receptor coactivators lysine-specific histone demethylase 1 and four and a half LIM domain protein 2 predict risk of prostate cancer recurrence. Cancer Res. *66*, 11341–11347.

Kim, J., Woo, A.J., Chu, J., Snow, J.W., Fujiwara, Y., Kim, C.G., Cantor, A.B., and Orkin, S.H. (2010). A Myc network accounts for similarities between embryonic stem and cancer cell transcription programs. Cell *143*, 313–324.

Kim, T., and Buratowski, S. (2009). Dimethylation of H3K4 by Set1 recruits the Set3 histone deacetylase complex to 5′ transcribed regions. Cell *137*, 259–272.

Krivtsov, A.V., Twomey, D., Feng, Z., Stubbs, M.C., Wang, Y., Faber, J., Levine, J.E., Wang, J., Hahn, W.C., Gilliland, D.G., et al. (2006). Transformation from committed progenitor to leukaemia stem cell initiated by MLL-AF9. Nature *442*, 818–822.

Lee, M.G., Wynder, C., Cooch, N., and Shiekhattar, R. (2005). An essential role for CoREST in nucleosomal histone 3 lysine 4 demethylation. Nature *437*, 432–435.

Lee, T.I., Jenner, R.G., Boyer, L.A., Guenther, M.G., Levine, S.S., Kumar, R.M., Chevalier, B., Johnstone, S.E., Cole, M.F., Isono, K., et al. (2006). Control of developmental regulators by Polycomb in human embryonic stem cells. Cell *125*, 301–313.

Lim, S., Janzer, A., Becker, A., Zimmer, A., Schüle, R., Buettner, R., and Kirfel, J. (2010). Lysine-specific demethylase 1 (LSD1) is highly expressed in ER-negative breast cancers and a biomarker predicting aggressive biology. Carcinogenesis *31*, 512–520.

Lin, C., Smith, E.R., Takahashi, H., Lai, K.C., Martin-Brown, S., Florens, L., Washburn, M.P., Conaway, J.W., Conaway, R.C., and Shilatifard, A. (2010). AFF4, a component of the ELL/P-TEFb elongation complex and a shared subunit of MLL chimeras, can link transcription elongation to leukemia. Mol. Cell *37*, 429–437.

Metzger, E., Wissmann, M., Yin, N., Müller, J.M., Schneider, R., Peters, A.H., Günther, T., Buettner, R., and Schüle, R. (2005). LSD1 demethylates repressive histone marks to promote androgen-receptor-dependent transcription. Nature *437*, 436–439.

Muntean, A.G., Tan, J., Sitwala, K., Huang, Y., Bronstein, J., Connelly, J.A., Basrur, V., Elenitoba-Johnson, K.S., and Hess, J.L. (2010). The PAF complex synergizes with MLL fusion proteins at HOX loci to promote leukemogenesis. Cancer Cell *17*, 609–621.

Nakamura, T., Mori, T., Tada, S., Krajewski, W., Rozovskaia, T., Wassell, R., Dubois, G., Mazo, A., Croce, C.M., and Canaani, E. (2002). ALL-1 is a histone methyltransferase that assembles a supercomplex of proteins involved in transcriptional regulation. Mol. Cell *10*, 1119–1128.

Ram, O., Goren, A., Amit, I., Shoresh, N., Yosef, N., Ernst, J., Kellis, M., Gymrek, M., Issner, R., Coyne, M., et al. (2011). Combinatorial patterning of chromatin regulators uncovered by genome-wide location analysis in human cells. Cell *147*, 1628–1639.

Saleque, S., Kim, J., Rooke, H.M., and Orkin, S.H. (2007). Epigenetic regulation of hematopoietic differentiation by Gfi-1 and Gfi-1b is mediated by the cofactors CoREST and LSD1. Mol. Cell *27*, 562–572.

Sanz, M.A., and Lo-Coco, F. (2011). Modern approaches to treating acute promyelocytic leukemia. J. Clin. Oncol. *29*, 495–503.

Schulte, J.H., Lim, S., Schramm, A., Friedrichs, N., Koster, J., Versteeg, R., Ora, I., Pajtler, K., Klein-Hitpass, L., Kuhfittig-Kulle, S., et al. (2009). Lysine-specific demethylase 1 is strongly expressed in poorly differentiated neuroblastoma: implications for therapy. Cancer Res. *69*, 2065–2071.

Shi, Y., Lan, F., Matson, C., Mulligan, P., Whetstine, J.R., Cole, P.A., Casero, R.A., and Shi, Y. (2004). Histone demethylation mediated by the nuclear amine oxidase homolog LSD1. Cell *119*, 941–953.

Singh, M.M., Manton, C.A., Bhat, K.P., Tsai, W.W., Aldape, K., Barton, M.C., and Chandra, J. (2011). Inhibition of LSD1 sensitizes glioblastoma cells to histone deacetylase inhibitors. Neuro-oncol. *13*, 894–903.

Somervaille, T.C., and Cleary, M.L. (2006). Identification and characterization of leukemia stem cells in murine MLL-AF9 acute myeloid leukemia. Cancer Cell *10*, 257–268.

Somervaille, T.C., Matheny, C.J., Spencer, G.J., Iwasaki, M., Rinn, J.L., Witten, D.M., Chang, H.Y., Shurtleff, S.A., Downing, J.R., and Cleary, M.L. (2009). Hierarchical maintenance of MLL myeloid leukemia stem cells employs a transcriptional program shared with embryonic rather than adult stem cells. Cell Stem Cell *4*, 129–140.

Subramanian, A., Tamayo, P., Mootha, V.K., Mukherjee, S., Ebert, B.L., Gillette, M.A., Paulovich, A., Pomeroy, S.L., Golub, T.R., Lander, E.S., and Mesirov, J.P. (2005). Gene set enrichment analysis: a knowledge-based approach for interpreting genome-wide expression profiles. Proc. Natl. Acad. Sci. USA *102*, 15545–15550.

Wang, J., Scully, K., Zhu, X., Cai, L., Zhang, J., Prefontaine, G.G., Krones, A., Ohgi, K.A., Zhu, P., Garcia-Bassets, I., et al. (2007). Opposing LSD1 complexes function in developmental gene activation and repression programmes. Nature *446*, 882–887.

Yokoyama, A., Lin, M., Naresh, A., Kitabayashi, I., and Cleary, M.L. (2010). A higher-order complex containing AF4 and ENL family proteins with P-TEFb facilitates oncogenic and physiologic MLL-dependent transcription. Cancer Cell *17*, 198–212.

Zuber, J., Rappaport, A.R., Luo, W., Wang, E., Chen, C., Vaseva, A.V., Shi, J., Weissmueller, S., Fellmann, C., Taylor, M.J., et al. (2011a). An integrated approach to dissecting oncogene addiction implicates a Myb-coordinated self-renewal program as essential for leukemia maintenance. Genes Dev. *25*, 1628–1640.

Zuber, J., Shi, J., Wang, E., Rappaport, A.R., Herrmann, H., Sison, E.A., Magoon, D., Qi, J., Blatt, K., Wunderlich, M., et al. (2011b). RNAi screen identifies Brd4 as a therapeutic target in acute myeloid leukaemia. Nature *478*, 524–528.